AGU PUBLICATIONS

JGR

Journal of Geophysical Research: Space Physics

RESEARCH ARTICLE

10.1002/2016JA022406

Special Section:

Inner Magnetosphere Coupling: Recent Advances

Key Points:

- The FPRs associated with the dipolarization front and substorm dipolarization are presented
- Behind the DF the electron quasi-perpendicular and field-aligned distributions are observed
- The features of betatron and Fermi acceleration are also observed during substorm dipolarization

Correspondence to:
C. L. Tang,
tcl@sdu.edu.cn

Citation:
Tang, C. L., M. Zhou, Z. H. Yao, and F. Shi (2016), Electron acceleration associated with the magnetic flux pileup regions in the near-Earth plasma sheet: A multicase study, *J. Geophys. Res. Space Physics*, *121*, 4331–4342, doi:10.1002/2016JA022406.

Received 5 JUL 2015
Accepted 28 APR 2016
Accepted article online 1 MAY 2016
Published online 17 MAY 2016

Electron acceleration associated with the magnetic flux pileup regions in the near-Earth plasma sheet: A multicase study

C. L. Tang[1], M. Zhou[2], Z. H. Yao[3], and F. Shi[4]

[1]Shandong Provincial Key Laboratory of Optical Astronomy and Solar-Terrestrial Environment, Institute of Space Sciences, Shandong University, Weihai, China, [2]Institute of Space Science and Technology, Nanchang University, Nanchang, China, [3]UCL Mullard Space Science Laboratory, Dorking, UK, [4]Physics and Space Sciences, Florida Institute of Technology, Melbourne, Florida, USA

Abstract Using the Time History of Events and Macroscale Interactions during Substorms (THEMIS) observations, we study electron acceleration (<30 keV) in the magnetic flux pileup regions (FPRs) in the near-Earth plasma sheet ($X \sim -10\ R_E$). We present three cases of FRPs associated with dipolarization fronts and substorm dipolarization. Based on the characteristics of the magnetic field, we defined the magnetic field enhancement region (MFER) as the magnetic field with significant ramp that is usually observed near the dipolarization front boundary layer. On the other side, the increased magnetic field without a significant ramp is the rest of a FPR. Our results show that betatron acceleration dominates for 10–30 keV electrons inside the MFER, whereas Fermi acceleration dominates for 10–30 keV electrons inside the rest of the FPR. Betatron acceleration is caused by the enhancement of the local magnetic field, whereas Fermi acceleration is related to the shrinking length of magnetic field line. These accelerated electrons inside the FPRs in the near-Earth tail play a potentially important role in the evolution of the Earth's electron radiation belt and substorms.

1. Introduction

The magnetic flux pileup region (FPR) in the near-Earth plasma sheet is very important to the study of magnetospheric substorms. Generally, in the near-Earth tail, there are two types of dipolarization that are associated with the form of the FPR. One dipolarization is characterized by a temporary increase in the magnetic field B_z component (or the dipolarization front, DF), whereas the other shows a prolonged increase in the B_z component (or substorm dipolarization) [*Nakamura et al.*, 2009; *Lui*, 2011; *Yao et al.*, 2012]. The former one is often observed in the magnetotail during the bursty bulk flow (BBF) events [*Birn et al.*, 2011; *Nakamura et al.*, 2002, 2009; *Runov et al.*, 2009; *Sitnov et al.*, 2009; *Tang et al.*, 2010; 2013; *Zhou et al.*, 2009]. DF is an ion gyroscale boundary between the ambient plasma sheet and the dipolarization flux tube [*Runov et al.*, 2011]. Although two mechanisms, i.e., flow braking and impulsive reconnection, are suggested to form DF, it is not necessity for these two processes to generate DF. Strictly speaking, the injection of an underpopulated flux tube is essential in forming a DF [e.g., *Birn et al.*, 2004; *Pritchett and Coroniti*, 2011]. The region of high magnetic field behind the DF is collectively named FPR [*Khotyaintsev et al.*, 2011; *Fu et al.*, 2011]. The high B_z region behind the DF contains significant magnetic flux, which is also referred to a dipolarizing flux bundle [*Liu et al.*, 2013]. In this paper, we use the term FPRs when referring to enhanced magnetic flux regions. The energetic electrons are usually observed inside the FPR behind the DF [e.g., *Fu et al.*, 2011]. There are various mechanisms responsible for electron acceleration associated with DFs, which mainly include adiabatic betatron acceleration and Fermi acceleration [*Wu et al.*, 2006; *Ashour-Abdalla et al.*, 2011; *Fu et al.*, 2011; *Birn et al.*, 2013; *Zhou et al.*, 2013; *Tang et al.*, 2013] and nonadiabatic acceleration [*Zhou et al.*, 2009; *Deng et al.*, 2010; *Khotyaintsev et al.*, 2011; *Huang et al.*, 2012]. Using Cluster data, *Fu et al.* [2012] statistically examined the pitch angle distribution (PAD) of >40 keV electrons inside the FPRs behind the DFs and found that the local velocity of the flux tubes determined the electron PADs. Based on the Time History of Events and Macroscale Interactions (THEMIS) data [*Angelopoulos*, 2008], *Wu et al.* [2013] statistically studied the electron (>30 keV) acceleration associated with the DFs and found that betatron acceleration and Fermi acceleration dominated in approximately 46% and 39% of the DF events in the near-Earth plasma sheet, respectively.

The latter type of dipolarization (substorm dipolarization) is associated with the development of substorm current wedge (SCW) [e.g., *McPherron et al.*, 1973; *Lui*, 1996], which is also observed by THEMIS probes in

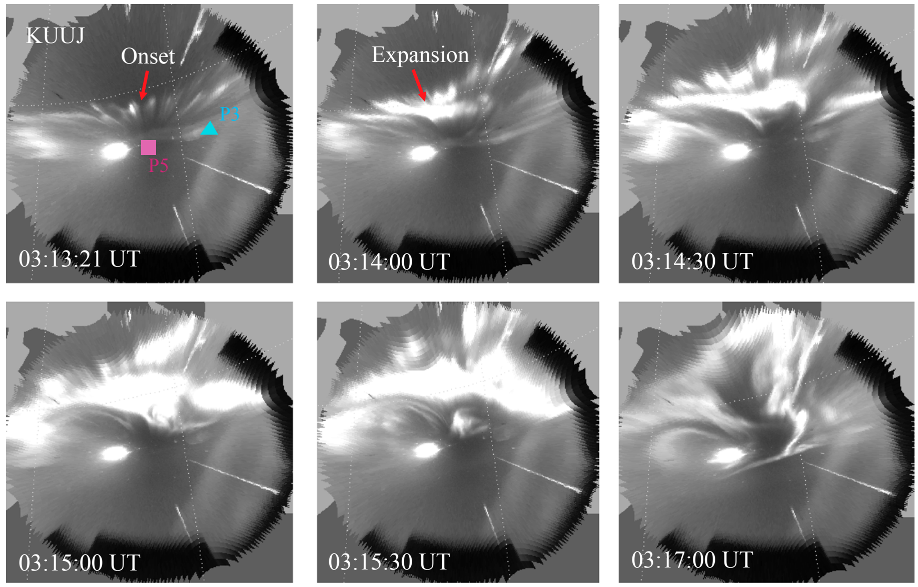

Figure 1. THEMIS all-sky camera images from the selected times to show the main auroral features of the substorm on 5 March 2009. The station used in the figure is Kuujjuaq (KUUJ, longitude: 291.6°; latitude: 58.1°). Red arrows indicate the auroral activations of interest referred to in the text.

the near-Earth tail [*Tang et al.*, 2009; *Lee et al.*, 2012; *Tang et al.*, 2013]. The electron injection associated with substorm dipolarization is one of the typical substorm signatures [e.g., *Lezniak and Winckler*, 1970]. Compared to the dipolarization timescale (tens of seconds to minutes), the energetic electrons in the plasma sheet have a small gyroperiod ($T_g \sim 10^{-3}$ s) and a small bouncing period ($T_b \sim 1$ s). These energetic electrons should conserve their first and second adiabatic invariants during the dipolarization process. The magnetic field strength in the near-Earth tail during substorm dipolarization can have a strong enhancement, which could lead to betatron acceleration in the near-Earth magnetotail [e.g., *Wu et al.*, 2006]. The substorm dipolarization corresponds to reconfiguration of the magnetic field topology, which could lead to the shrinking length of the magnetic field line [e.g., *Birn et al.*, 2004, 2013]. The shortened magnetic field line could lead to Fermi acceleration [e.g., *Deng et al.*, 2010]. *Asano et al.* [2010] have shown that the parallel fluxes for the energetic electrons (20–200 keV) exceed the perpendicular fluxes during substorm dipolarization. The near 90° PADs for the 30–200 keV electrons were observed during the tailward propagating dipolarization, which was suggested to be a result of a local compression of the magnetic field [*Tang et al.*, 2013].

In order to better understand the electron acceleration (<30 keV) associated with the FPRs in the near-Earth tail ($X \sim -10\ R_E$), we examine the electron PADs inside the FPRs in this paper. The three events of FPRs associated with the DF and substorm dipolarization are presented.

2. THEMIS Observations

2.1. The 5 March 2009 Event

The 5 March 2009 event is examined in detail in the present study. High-resolution (3 s) all-sky images available from the Kuujjuaq (KUUJ) station from 0313:21 UT to 0317:00 UT on 5 March 2009 are shown in Figure 1. The mapping foot points of the satellites according to the T96 magnetospheric model [*Tsyganenko*, 1995] suggest that the two THEMIS probes (P3 and P5) were located around the KUUJ station, and the proximate ionospheric foot point of P3 was poleward of P5. At 0313:21 UT, the substorm expansion onset with a wave-like structure was clearly observed at KUUJ station, while the poleward auroral expansion was observed at the Narsarsuaq (NRSQ) station (not shown). After 0314:00 UT, a farther poleward auroral expansion was observed at the KUUJ station.

Figures 2 and 3 summarize the magnetic field and plasma signatures of FPRs in the near-Earth tail observed by P3 and P5, respectively, on 5 March 2009. P3 detected a small $|B_x|$ (Figure 2a), indicating that P3 was near

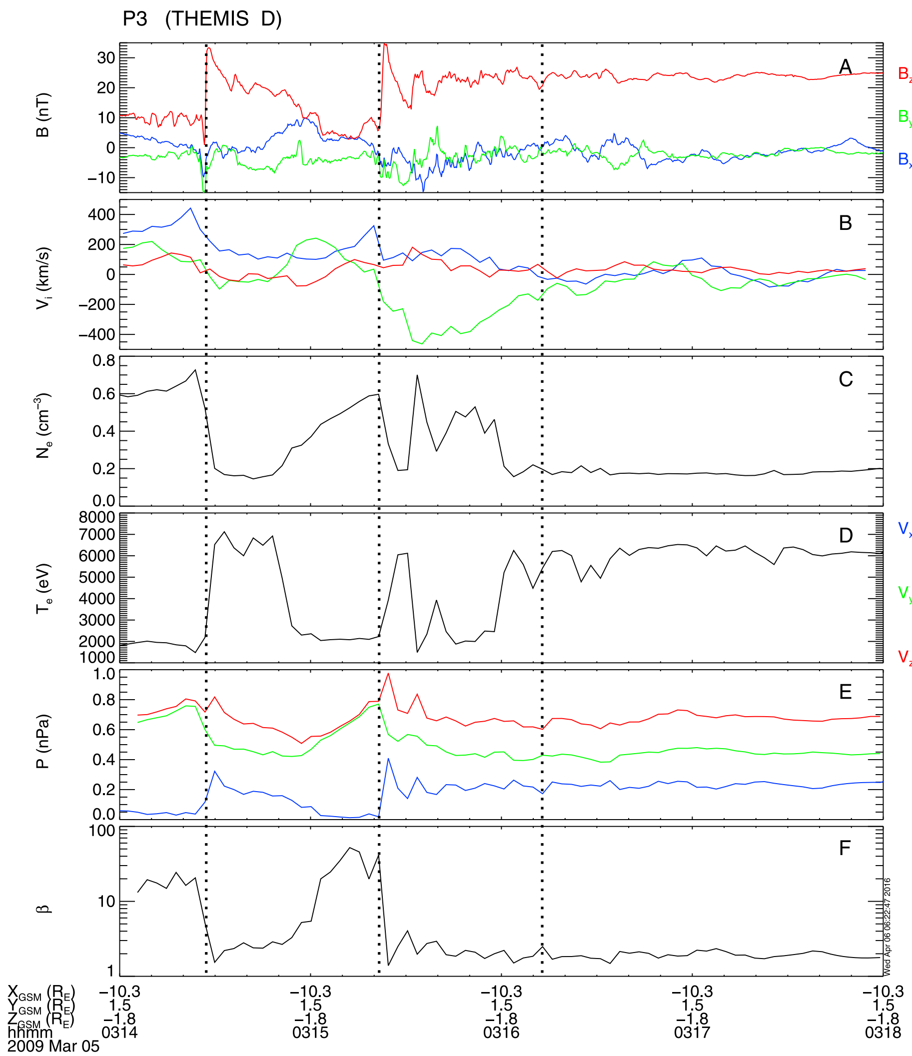

Figure 2. Summary of P3 (THEMIS D) observations during the time interval from 0314 to 0318 UT on 5 March 2009. The figures are (a) the magnetic field **B**, (b) the ion flow velocity V_i, (c) the electron number density N_e, (d) the electron temperature T_e, (e) the pressures (the magnetic pressure P_m, the plasma pressure P_p, and the total (plasma plus magnetic) pressure P_t), and (f) β (the ratio of the plasma pressure to the magnetic pressure). Note that the ion flow velocity V_i, electron number density N_e, and electron temperature T_e are provided by combining the measurements from both the ESA and SST instruments. The vertical dashed lines indicate the times of the DFs and substorm dipolarization at P3.

the neutral sheet. The B_x component at P5 was ~ −20 nT (Figure 3a), which indicates that P5 was below the neutral sheet in the outer plasma sheet. The first DF was successively observed by P3 at ~ 0314:27 UT (indicated by the first vertical dashed line in Figure 2) and then by P5 at ~ 0314:34 UT (indicated by the first vertical dashed line in Figure 3), which has been identified by *Li et al*. [2011] and *Runov et al*. [2011]. The first DF observed by P3 was associated with the braked earthward moving flows as shown in Figure 2b. Note that the pronounced compression region (P_p and P_t increased) was observed by P3 ahead the first DF (Figure 2 e), in agreement with the simulation study [*Yang et al*., 2011]. The DF at P5 had a sharp leading boundary and a sharp trailing boundary, which were similar to the observations in *Zhou et al*. [2013]. Figure 3b shows that the DF at P5 was associated with the dawnward flows. Similar ion flows have been observed by *Keiling et al*. [2009] and *Panov et al*. [2010]. P3 detected the second DF at ~ 0315:22 UT (indicated by the second vertical dashed line in Figure 2), which was also associated with the dawnward flows. At 0315:45 UT, P4 (THEMIS E, ~ 0.7 R_E northward of P5) also observed the second DF (not shown). However, P5 did not observe the second DF, which was consistent with the limited scale in the N-S direction of the fast flows (~2 R_E) in the plasma sheet [*Nakamura et al*., 2004]. These also showed that the FPRs associated with the DFs were localized.

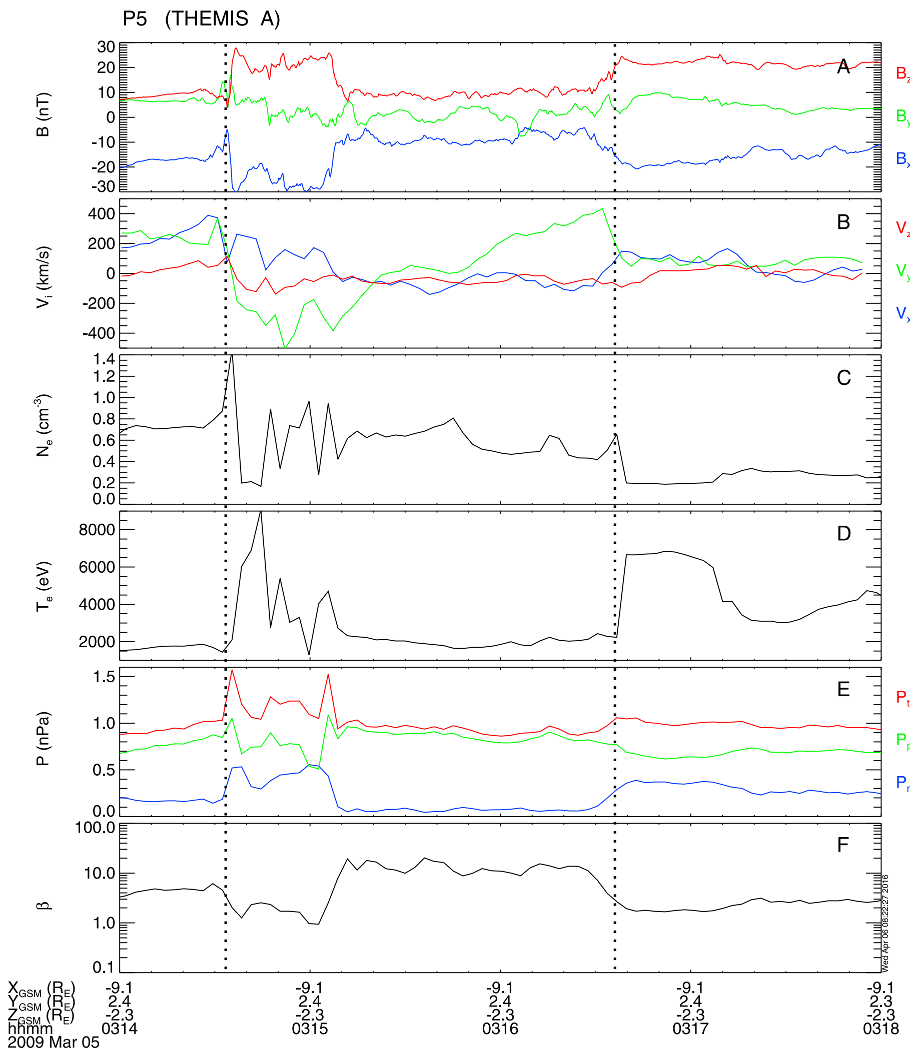

Figure 3. Summary of P5 (THEMIS A) observations during the time interval from 0314 to 0318 UT on 5 March 2009. The format is the same as in Figure 2.

These DFs observed by the THEMIS probes (P3 and P5) were associated with a decrease in the local electron number density N_e and electron temperature T_e enhancement (Figures 2c, 2d, 3c, and 3d). After some magnetic field fluctuations, the B_z component at P3 reached a stable level after ~ 0316:12 UT (indicated by the third vertical dashed line in Figure 2). P5 also observed the increases in the B_z component and braked flows at 0316:36 UT (indicated by the second vertical dashed line in Figure 3). The plasma number density N_e decreased (Figure 3c) and plasma temperature T_e clearly increased (Figure 3d). Subsequently, the elevation angle of the local magnetic field increased (not shown), and the magnetic field configuration in the near-Earth tail became more dipolar. These were the characteristics of substorm dipolarization.

Figures 4 and 5 show the magnetic field **B**, the total magnetic field B_t, the electron PADs in the electrostatic analyzer (ESA) energy range (1–30 keV), and the onboard electric field wave power spectral density during the time interval from 0314 to 0318 UT on 5 March 2009 obtained by P3 and P5, respectively. The scale on the *y* axis gives the pitch angles with 180° (antiparallel) at the top and 0° (parallel) at the bottom of each panel. Behind the first DF (indicated by the first vertical dashed line in Figure 4), P3 first observed the quasi-perpendicular distributions (near 90°) (indicated by the shaded gray area in Figures 4e and 4f) and then the field-aligned distributions (near 0° and 180°) for electrons of energy greater than 10 keV (indicated by the shaded purple red area in Figures 4e and 4f). P3 mainly observed the field-aligned distributions for >10 keV electrons behind the second DF (indicated by the second vertical dashed line in Figure 4). These quasi-perpendicular distributions for

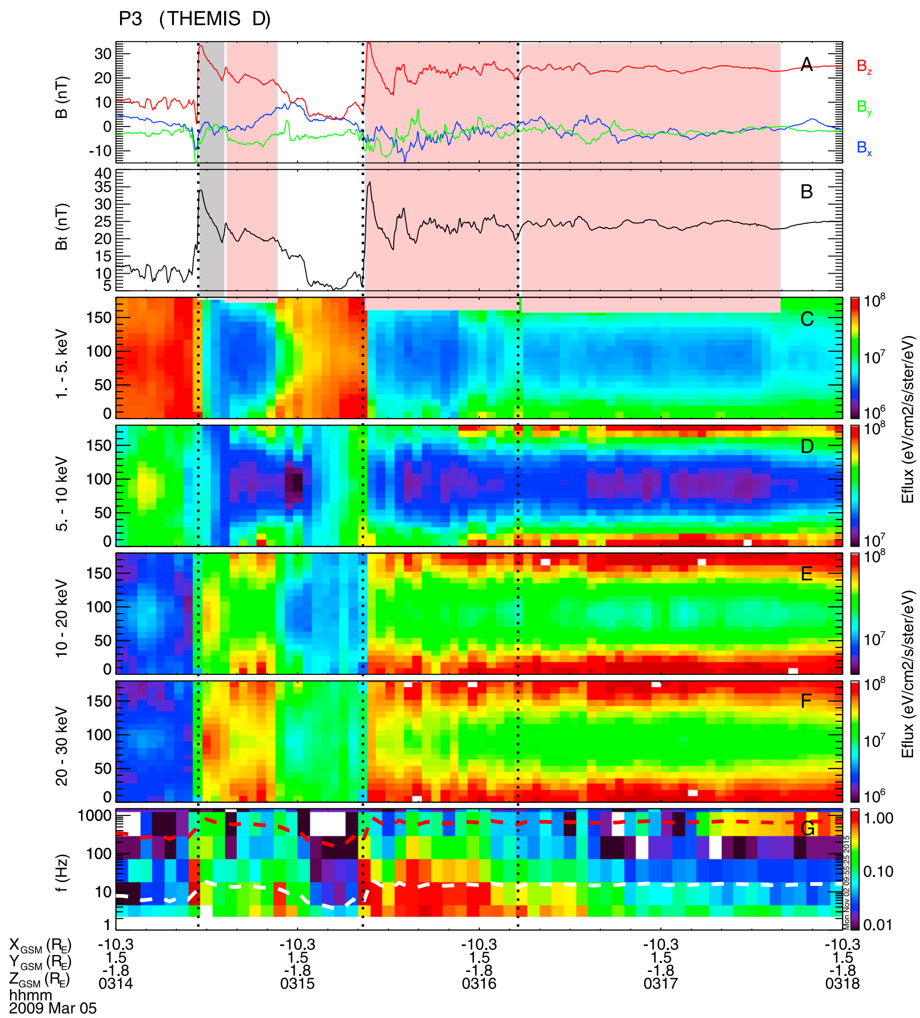

Figure 4. Observations from P3 (THEMIS D) during the time interval from 0314 to 0318 UT on 5 March 2009. (a) the magnetic field **B**, (b) the total magnetic field B_t, (c–f) the electron energy flux variation in the ESA energy range (1–30 keV) as a function of pitch angle, and (g) the electric field wave power spectral density. The superimposed dashed traces are at the electron cyclotron frequency (red) and the lower hybrid frequency (white). The vertical dashed lines indicate the times of the DFs and substorm dipolarization at P3. The shaded gray and purple red areas indicate the quasi-perpendicular and quasi-parallel distributions for >10 keV electrons, respectively.

>10 keV electrons behind the first DF at P3 could be attributed to betatron acceleration. The enhanced magnetic field was observed between 0314:28 UT and 0314:38 UT (indicated by the shaded gray area in Figure 4b). Enhancements of quasi-parallel fluxes for >10 keV electrons at P3 behind the DFs and during substorm dipolarization (indicated by the shaded purple red areas in Figures 4e and 4f) could be attributed to Fermi acceleration, which may be related to the shrinking length of magnetic field line.

P5, which was located at the duskside of P3, also observed enhancements of quasi-parallel fluxes for >10 keV electrons behind the first DF (indicated by the shaded purple red area in Figures 5e and 5f). During the substorm dipolarization (indicated by the second vertical dashed line in Figure 5), P5 first observed enhancements of quasi-perpendicular fluxes for >10 keV electrons after 0316:36 UT (indicated by the shaded gray area in Figures 5e and 5f) and then enhancements of quasi-parallel fluxes after 0317:40 UT (indicated by the shaded purple red area in Figures 5e and 5f). These quasi-perpendicular distributions >10 keV electrons at P5 were the features of betatron acceleration, which was caused by an enhanced magnetic field (indicated by the shaded gray area in Figure 5b) [*Northrop*, 1963]. The quasi-parallel distributions for >10 keV electrons at P5 were the features of Fermi acceleration, which was related to the shrinking length of magnetic field line during the dipolarization process.

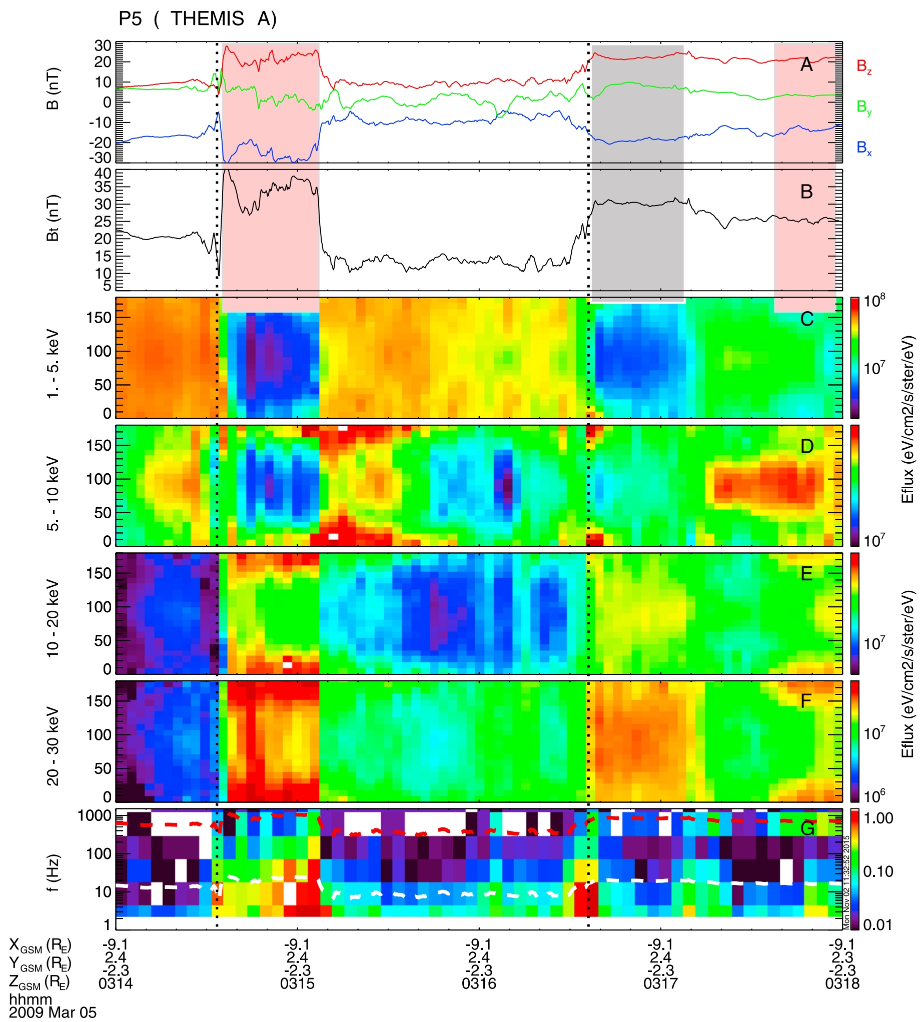

Figure 5. Observations from P5 (THEMIS A) during the time interval from 0314 to 0318 UT on 5 March 2009. The format is the same as in Figure 4.

Figure 6 shows the detailed electron PADs during the time interval from 0314 to 0317 UT on 5 March 2009 for 10 different energy channels from 0.43 keV to 26.4 keV observed by P3. Before the first DF (at 0314:11 UT), the PADs with 2.93–26.4 keV electrons peaked at approximately 90°. Behind the DF (at 0314:32 UT), the phase space density (PSD) of the lower energy (<5.0 keV) electrons decreased dramatically, whereas the PSD of the higher energies (>15.0 keV) increased by over an order of magnitude. The PSD increases peaked at approximately 90° pitch angle. At 0314:45 UT, the electrons (<5.0 keV) had a cigar distribution with peaks at ~ 0° and 180° pitch angles, and the PSD of >5.0 keV electrons at ~ 0° and 180° pitch angles increased inside the FPR. The PADs of electrons (2.93–26.4 keV) were nearly isotropic at 0315:09 UT, whereas the PSD of the higher energies (>5.0 keV) increased with peaks at ~ 0° and 180° pitch angles at 0315:24 UT. During the substorm dipolarization (after 0316:31 UT), the electrons had a clear cigar distribution with peaks at ~ 0° and 180° pitch angles.

2.2. The 14 February 2008 Event

The expansion phase onset of a small substorm occurred at ~ 0246 UT on 14 February 2008, which was indicated by the THEMIS *AE* index (not shown). The DF followed by substorm dipolarization at ~ 0245 UT was observed by P3, which is not shown because our major concern is to understand the electron dynamics of the FPR associated with the DF. Figure 7 summarizes the magnetic field and plasma measurements of the FPR in the near-Earth tail observed by P3 for this event. P3 detected a small $|B_x|$ (<10 nT), which indicates that P3 was also located in the central plasma sheet. The DF was observed by P3 at ~ 0244:29 UT (indicated by the vertical dashed line in Figure 7), which was associated with the slow earthward moving flows,

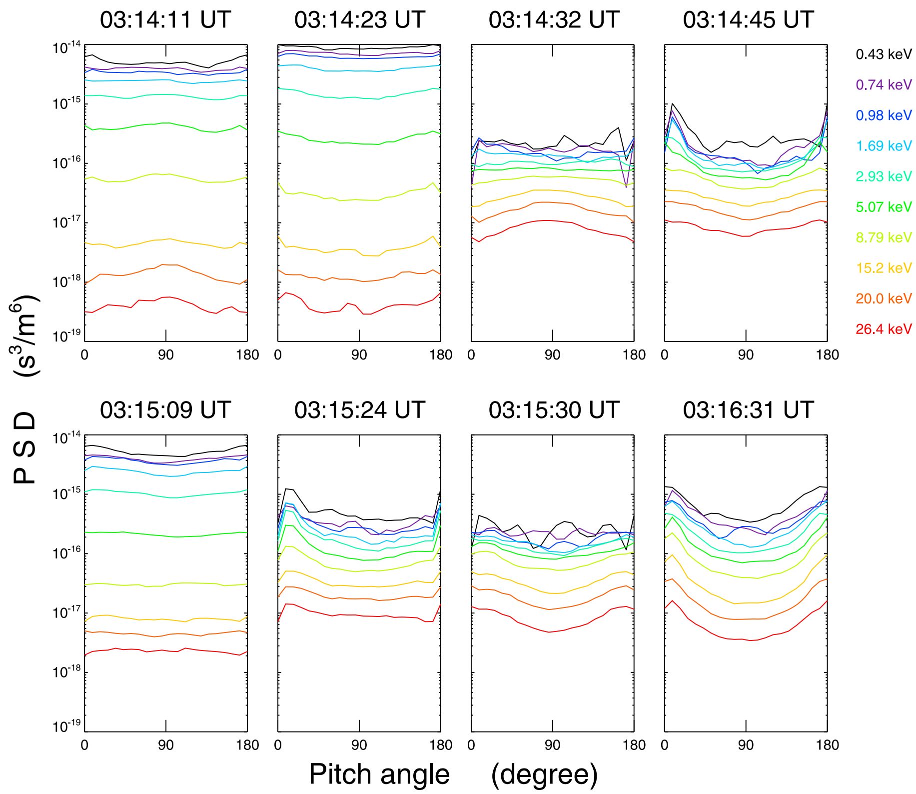

Figure 6. The detailed PADs are shown from P3 during the time interval from 0314 to 0317 UT on 5 March 2009 for 10 different energy channels from 0.43 keV to 26.4 keV.

as shown in Figure 7c. The electron number density N_e associated with the DF initially increased, followed by a decrease after the B_z component peak (Figure 7d), whereas the electron temperature T_e changed in an opposite trend (not shown). The plasma pressure P_p decreased after the arrival of the front, whereas the magnetic pressure P_m increased at the front and returned to the initial value within ~ 20 s behind the DF. The total pressure P_t increased behind the front because of the increase in P_m (Figure 7e). At ~ 0244 UT, P4 (THEMIS E, ~ 1.2 R_E earthward of P3) did not observe this DF (not shown). Behind the DF, P3 first observed the quasi-perpendicular distributions (indicated by the shaded gray area in Figures 7f and 7g) and then the quasi-parallel distributions for $>$10 keV electrons (indicated by the shaded purple red area in Figures 7f and 7g). Enhancements of quasi-perpendicular fluxes for more than 10 keV electrons at P3 is likely attributed to betatron acceleration, for which an enhanced magnetic field was observed between 0244:29 UT and 0244:38 UT (indicated by the shaded gray area in Figure 8b). Enhancements of quasi-parallel fluxes for $>$10 keV electrons at P3 after 0244:38 UT is likely attributed to Fermi acceleration.

2.3. The 27 March 2008 Event

A large substorm occurred at 0729 UT on 27 March 2008, as indicated by the THEMIS *AE* index (not shown). At ~ 0729 UT, an auroral brightening first appeared; subsequently, the poleward expansion of aurora was detected at Gillam (GILL) station. Figure 8 summarizes the magnetic field and plasma measurements of the FPR associated with the DF in the near-Earth tail observed by P3 on 27 March 2008. P3 was located near the neutral sheet and observed a small B_x ($|B_x| < 10$ nT). The DF was observed by P3 at ~ 0730:10 UT (indicated by the vertical dashed line in Figure 8), which was associated with the slow earthward and dawnward flows, as shown in Figure 8c. The electron number density N_e decreased behind the DF (Figure 8d), whereas the electron temperature T_e increased (not shown). The plasma pressure P_p decreased behind the DF. The magnetic pressure P_m increased at the front and returned to the initial value within ~ 22 s. The change of the total pressure P_t was in accord with that of P_m (Figure 8e). Behind the DF, P3 first observed the quasi-perpendicular distributions (indicated by the shaded gray area in Figures 8f and 8g) and then the field-aligned distributions for more than 10 keV electrons (indicated by the shaded purple red area in Figures 8f and 8g). The quasi-perpendicular

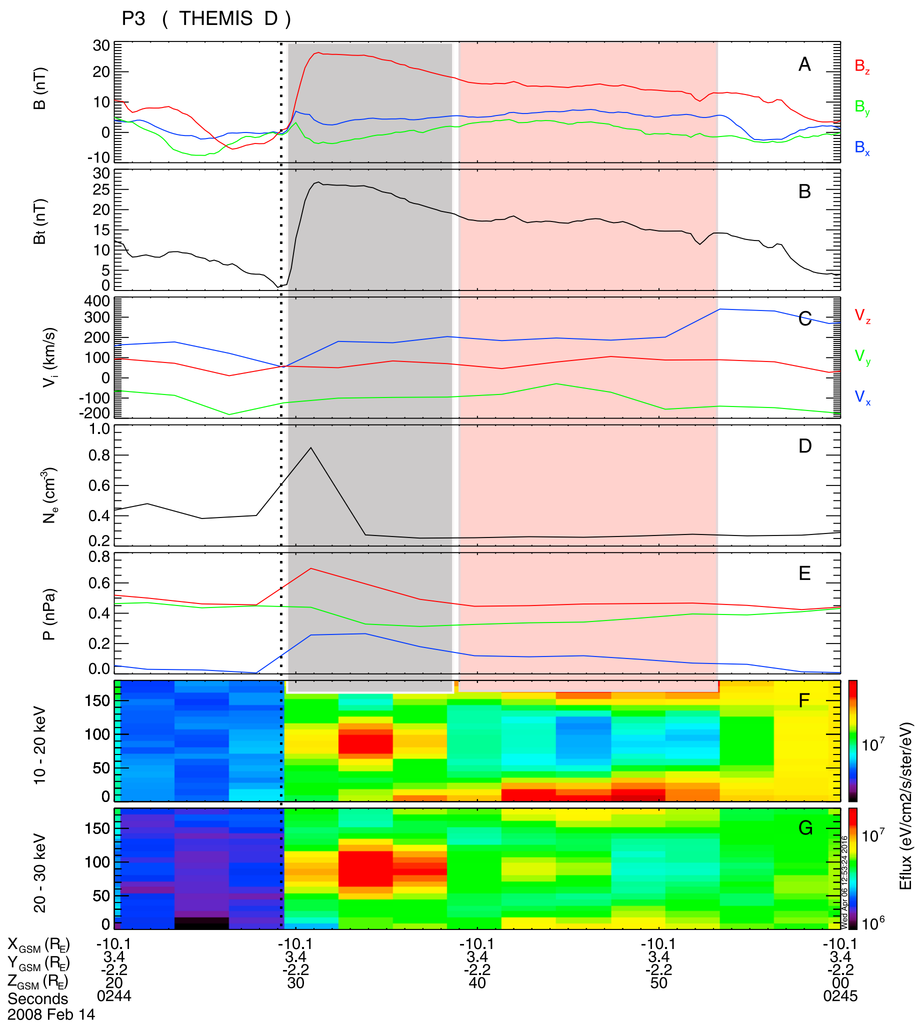

Figure 7. Observations from P3 (THEMIS D) during the time interval from 0244:20 to 0245:00 UT on 14 February 2008. (a) the magnetic field **B**, (b) the total magnetic field B_t, (c) the ion flow velocity V_i, (d) the electron number density N_e, (e) the pressures (the magnetic pressure P_m, the plasma pressure P_p, and the total (plasma plus magnetic) pressure P_t), and (f and g) the electron energy flux variation in the ESA energy range (10–30 keV) as a function of pitch angle. Note that the ion flow velocity V_i and electron number density N_e are provided by combining the measurements from both the ESA and SST instruments. The vertical dashed line indicates the time of the DF. The shaded gray and purple red areas indicate the quasi-perpendicular and quasi-parallel distributions for >10 keV electrons, respectively.

distributions for >10 keV electrons at P3 could be attributed to betatron acceleration, for which an enhanced magnetic field was observed between 0730:12 UT and 0730:22 UT (indicated by the shaded gray area in Figure 8b). The quasi-parallel distributions for >10 keV electrons at P3 between 0730:24 UT and 0730:36 UT could be attributed to Fermi acceleration.

3. Discussion and Summary

We examined the electron acceleration (<30 keV) associated with the FPRs in the near-Earth tail ($X \sim -10\, R_E$) using THEMIS observations. The common electron dynamic features of FPRs associated with DF and substorm dipolarization were presented in all the three events. The main results are summarized as follows.

1. A magnetic field enhancement region (MFER) is usually formed in the localized FPR associated with the DF (Figure 9a). Inside the MFER, the B_z component increases sharply and quasi-perpendicular distributions dominate for 10–30 keV electrons, which is a feature of betatron acceleration. Inside the rest of the FPR, the B_z component either remains at the increased level or slowly decreases (as a function of time or redial distance) and quasi-parallel distributions dominate for 10–30 keV electrons, which is a feature of Fermi acceleration.

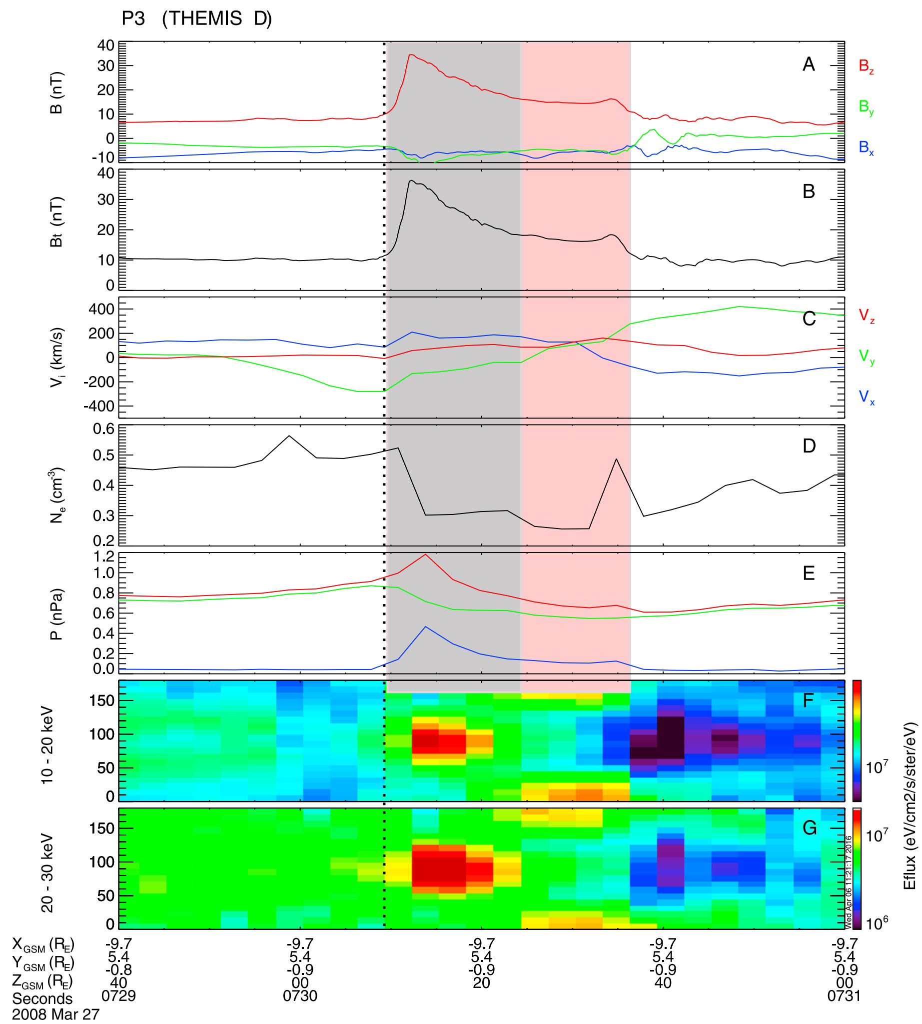

Figure 8. Observations from P3 (THEMIS D) during the time interval from 0729 to 0731 UT on 27 March 2008. The format is the same as in Figure 7.

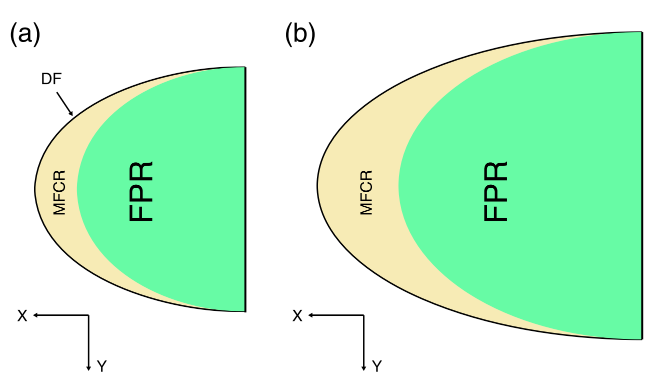

Figure 9. A schematic to illustrate the magnetic FPRs in the near-Earth plasma sheet in the equatorial plane: (a) the localized FPR associated with the DFs and (b) the large-scale FPR associated with substorm dipolarization. The pale goldenrod region is the MFER; the pale green region indicates the rest of the FPR.

2. Another phenomenon is that the MFER in the large-scale FPR associated with substorm dipolarization (Figure 9b) in which the feature of betatron acceleration for 10–30 keV electrons was observed. Inside the rest of the FPR, the feature of Fermi acceleration for 10–30 keV electrons was observed.

Simple calculations based on the P3 observations of the 5 March 2009 event were conducted in order to quantify the adiabatic acceleration (Fermi and betatron) to determine the main acceleration mechanisms for the electrons (<30 keV) inside the FPRs associated with the DFs and substorm dipolarization. Assuming that the electrons in the quiet near-Earth tail (e.g., 0314:23 UT panel in Figure 6) come from magnetic reconnection in the midtail ($L \sim 20$, L is McIlwain parameter), these electrons can be seen as the source population for the adiabatic acceleration. Inside the leading part of the FPR behind the first DF, the magnetic field strength $B_t^{'}$ was up to ~ 35 nT. If B_t was approximately 10 nT in the reconnection region in the midtail ($L \sim 20$), then $B_t^{'}/B_t$ was approximately 3.5. For betatron acceleration at $L \sim 10$, we obtained $E_{\perp}^{'} = \left(B_t^{'}/B_t\right)E_{\perp} = 3.5E_{\perp}$, where $E_{\perp}$ and $E_{\perp}^{'}$ indicate the electron energy in direction of the velocity V perpendicular to the magnetic field before and after the acceleration, respectively. For example, if the initial energy of the electrons was 5 keV, then the accelerated energy could be up to 15 keV. In the 0314:32 UT panel in Figure 6, the PSD of 15 keV electrons at ~ 90° pitch angle increased by 1 order of magnitude. Although the PSD of 15 keV electrons at ~ 0° and 180° pitch angles increased by a factor of 4, betatron acceleration dominated for 10–30 keV electrons inside the leading part of the FPR behind the first DF (or the MFER in the localized FPR associated with the DF). Based on similar considerations, betatron acceleration dominated over Fermi acceleration for 10–30 keV electrons inside the MFER in the large-scale FPR associated with substorm dipolarization at P5. *Li et al.* [2011] have shown that plasma acceleration behind the DF could be explained by the increased curvature force density due to the increase in the magnetic field. This explanation is consistent with our interpretations.

By calculating the ratio S/S', we can quantify Fermi acceleration in near-Earth tail ($L \sim 10$) (S and S' denote the magnetic field line length of the electrons location before and after dipolarization, respectively). Using the dipole magnetic field line equation of *Cravens* [1997], *Wu et al.* [2006] obtained $S' \approx 27.6\,R_E$ at $L \sim 10$. Using their analytical method [see *Wu et al.*, 2006, Figure 3], S was approximately 47.6 R_E at $L \sim 20$. Thus, we obtained $E_{\parallel}^{'} = \left(S/S^{'}\right)^2 E_{\parallel} = 3E_{\parallel}$, where $E_{\parallel}$ and $E_{\parallel}^{'}$ denote the electron energy in direction of the velocity V parallel to the magnetic field before and after the acceleration, respectively. For example, Fermi acceleration could energize 5 keV electrons to 15 keV. In the 0314:45 UT and 0316:31 UT panels in Figure 6, the PSD of 15 keV electrons at ~ 0° and 180° pitch angles had a factor of 10 to 20 increase, while the PSD of 15 keV electrons at ~ 90° pitch angle only increased by 5 times. Fermi acceleration dominated over betatron acceleration for 10–30 keV electrons inside the rear part of the FPR behind the first DF (or the rest of the localized FPR associated with the DF). Based on the same considerations, quasi-parallel distributions for 10–30 keV electrons inside the rest of the large-scale FPR associated with substorm dipolarization at P5 could be attributed to Fermi acceleration.

The present result showed the electron acceleration ($<$30 keV) associated with the FPRs associated with the DFs and substorm dipolarization in the near-Earth tail, which differed from the previous results. *Fu et al.* [2011] suggest that betatron acceleration dominates for $>$40 keV electrons inside a growing FPR (the DF is in front of the BBF peak), which is caused by an enhancement of the magnetic field. Fermi acceleration dominates inside a decaying FPR (the DF is behind the BBF peak), which is associated with the shrinking length of magnetic flux tubes. For the first DF in the 5 March 2009 case, *Li et al.* [2011] have clearly shown that $\mathbf{E} \times \mathbf{B}$ is very consistent with the observational ion bulk velocity; thus, it is likely that the DF was traveling with the bulk flow rather than locally generated. According to the classifications of *Fu et al.* [2011], the FPR behind the DF (for example, the first DF observed by P3 at 0314:28 UT in the 5 March 2009 case) should be the "decaying FPR," and the electrons ($>$10 keV) inside the FPR behind the DF should exhibit Fermi acceleration. However, quasi-perpendicular and quasi-parallel distributions for 10–30 keV electrons were successively observed inside the same FPR associated with the DF. The quasi-perpendicular distributions for 10–30 keV electrons inside the MFER associated with the DF at P5 in the 5 March 2009 case were not observed, which may be due that these electrons were transported to the outer radiation belt (Figures 5e and 5f). *Runov et al.* [2013] have shown that pancake-type and cigar-type PADs coexist at the same DF. The pancake distribution is in the vicinity of the neutral sheet, and cigar type is above and below the neutral sheet. In our study, the electron PADs behind the DFs observed by P3 ($B_x \sim 0$ nT) in the three events were not consistent with the results of *Runov et al.* [2013].

Previous studies showed that betatron acceleration [*Wu et al.*, 2006] or Fermi acceleration [*Asano et al.*, 2010; *Deng et al.*, 2010] occurred in the near-Earth tail during the substorm dipolarization process. Because of the fortunate satellite location, P5 in the 5 March 2009 case provided a much better view of the large-scale FPR associated with substorm dipolarization than the previous studies could [e.g., *Wu et al.*, 2006; *Deng et al.*, 2010]. P5 observed the features of betatron acceleration and Fermi acceleration for 10–30 keV electrons inside the large-scale FPR associated with substorm dipolarization. The change from pancake- to cigar-type distribution may be due to the competition between betatron acceleration and Fermi acceleration. The magnetic field strength B_t corresponding to the pancake distribution was greater than that corresponding to the cigar distribution (Figure 5b). The factor of Fermi acceleration was more or less the same inside during the substorm dipolarization process, whereas the factor of betatron acceleration may vary significantly. Hence, betatron acceleration dominated inside the MFER. In the 5 March 2009 case, P3 (located in the tailward of P5) only observed the cigar-type distribution for 10–30 keV electrons during substorm dipolarization (Figures 4e and 4f).

Our observations have shown that the magnetized electrons in the near-Earth tail during dipolarization process may be accelerated by adiabatic affects. However, some studies have also shown that adiabatic acceleration was insufficient to account for the electron acceleration in the dipolarization process and that nonadiabatic acceleration was required [e.g., *Zhou et al*., 2009]. In the 5 March 2009 case, some wave enhancements occurred at P5 at near 0315:00 UT (Figure 5g), which may contribute to the flux enhancements for 10–30 keV electrons (Figure 5f). These waves may be important for nonadiabatic acceleration and pitch angle diffusion of the energetic electrons, although they are not discussed in detail here.

In the present study, we revealed the acceleration characteristics of the electrons (10–30 keV) inside the FPRs associated with the DFs and substorm dipolarization. These features depend to the relative location of the FPRs. Betatron acceleration is caused by enhancement of the local magnetic field, whereas Fermi acceleration is related to the shrinking length of magnetic field line. These accelerated electrons inside the FPRs play a potentially important role in the evolution of the Earth's electron radiation belt and substorms.

Acknowledgments
This work is supported by the National Natural Science Foundation of China grants 41004075, 41331068, and 41274170, the National Basic Research Program of China (2012CB825601), and the Shandong Province Natural Science Foundation of grant 2014ZRE27445. We thank V. Angelopoulos for use of data from the THEMIS Mission. We acknowledge the THEMIS investigators for the use of the data and the analysis software. Specifically, we thank C. W. Carlson and J. P. McFadden for ESA data, D. Larson and R. P. Lin for SST data, and K. H. Glassmeier, U. Auster, and W. Baumjohann for FGM data. All the data for this paper are available at the THEMIS data depository: http://themis.ssl.berkeley.edu/data/themis/.

References

Angelopoulos, V. (2008), The THEMIS mission, *Space Sci. Rev.*, *141*(1–4), 5–34, doi:10.1007/s11214-008-9336-1.

Asano, Y., et al. (2010), Electron acceleration signatures in the magnetotail associated with substorms, *J. Geophys. Res.*, *115*, A05215, doi:10.1029/2009JA014587.

Ashour-Abdalla, M., M. El-Alaoui, M. L. Goldstein, M. Zhou, D. Schriver, R. Richard, R. Walker, M. G. Kivelson, and K.-J. Hwang (2011), Observations and simulations of nonlocal acceleration of electrons in magnetotail magnetic reconnection events, *Nat. Phys.*, *7*, 360–365, doi:10.1038/NPHYS1903.

Birn, J., M. Thomsen, and M. Hesse (2004), Electron acceleration in thedynamic magnetotail: Test particle orbits in three-dimensional magneto-hydrodynamic simulation fields, *Phys. Plasmas*, *11*, 1825–1833.

Birn, J., R. Nakamura, E. V. Panov, and M. Hesse (2011), Bursty bulk flows and dipolarization in MHD simulations of magnetotail reconnection, *J. Geophys. Res.*, *116*, A01210, doi:10.1029/2010JA016083.

Birn, J., M. Hesse, R. Nakamura, and S. Zaharia (2013), Particle acceleration in dipolarization events, *J. Geophys. Res. Space Physics*, *118*, 1960–1971, doi:10.1002/jgra.50132.

Cravens, T. E. (1997), *Physics of Solar System Plasmas*, Cambridge Univ. Press, New York.

Deng, X., M. Ashour-Abdalla, M. Zhou, R. Walker, M. El-Alaoui, V. Angelopoulos, R. E. Ergun, and D. Schriver (2010), Wave and particle characteristics of earthward-moving electron injections associated with dipolarization fronts, *J. Geophys. Res.*, *115*, A09225, doi:10.1029/2009JA015107.

Fu, H. S., Y. V. Khotyaintsev, M. André, and A. Vaivads (2011), Fermi and betatron acceleration of suprathermal electrons behind dipolarization fronts, *Geophys. Res. Lett.*, *38*, L16104, doi:10.1029/2011GL048528.

Fu, H. S., Y. V. Khotyaintsev, A. Vaivads, M. André, V. A. Sergeev, S. Y. Huang, E. A. Kronberg, and P. W. Daly (2012), Pitch angle distribution of suprathermal electrons behind dipolarization fronts: A statistical overview, *J. Geophys. Res.*, *117*, A12221, doi:10.1029/2012JA018141.

Huang, S. Y., M. Zhou, X. H. Deng, Z. G. Yuan, Y. Pang, Q. Wei, W. Su, H. M. Li, and Q. Q. Wang (2012), Kinetic structure and wave properties associated with sharp dipolarization front observed by Cluster, *Ann. Geophys.*, *30*, 97–107, doi:10.5194/angeo-30-97-2012.

Keiling, A., et al. (2009), Substorm current wedge driven by plasma flow vortices: THEMIS observations, *J. Geophys. Res.*, *114*, A00C22, doi:10.1029/2009JA014114.

Khotyaintsev, Y. V., C. M. Cully, A. Vaivads, M. Andre, and C. J. Owen (2011), Plasma jet braking: Energy dissipation and nonadiabatic electrons, *Phys. Res. Lett.*, *106*(16), doi:10.1103/PhysRevLett.106.165001.

Lee, D.-Y., H.-S. Kim, S. Ohtani, and M. Y. Park (2012), Statistical characteristics of plasma flows associated with magnetic dipolarizations in the near-tail region of $r > 12\ R_E$, *J. Geophys. Res.*, *117*, A01207, doi:10.1029/2011JA017246.

Lezniak, T. W., and J. R. Winckler (1970), Experimental study of magnetospheric motions and the acceleration of energetic electrons during substorms, *J. Geophys. Res.*, *75*, 7075–7098, doi:10.1029/JA075i034p07075.

Li, S. S., V. Angelopoulos, A. Runov, X. Z. Zhou, J. McFadden, D. Larson, J. Bonnell, and U. Auster (2011), On the force balance around dipolarization fronts within bursty bulk flows, *J. Geophys. Res.*, *116*, A00I35, doi:10.1029/2010JA015884.

Liu, J., V. Angelopoulos, A. Runov, and X.-Z. Zhou (2013), On the current sheets surrounding dipolarizing flux bundles in the magnetotail: The case for wedgelets, *J. Geophys. Res. Space Physics*, *118*, 2000–2020, doi:10.1002/jgra.50092.

Lui, A. T. Y. (1996), Current disruption in the Earth's magnetosphere: Observations and models, *J. Geophys. Res.*, *101*, 13,067–13,088, doi:10.1029/96JA00079.

Lui, A. T. Y. (2011), Physical processes for magnetospheric expansion onsets, in *The Dynamic Magnetosphere, IAGA Spec. Sopron Book Ser*, vol. 3, edited by W. W. Liu and M. Fujiimoto, pp. 65–115, Springer, New York.

McPherron, R. L., C. T. Russell, and M. P. Aubry (1973), Satellite studies of magnetospheric substorms on August 15, 1968, 9. Phenomenological model for substorms, *J. Geophys. Res.*, *78*, 3131–3149, doi:10.1029/JA078i016p03131.

Nakamura, R., et al. (2002), Motion of the dipolarization front during a flow burst event observed by Cluster, *Geophys. Res. Lett.*, *29*(20), 1942, doi:10.1029/2002GL015763.

Nakamura, R., et al. (2004), Spatial scale of high-speed flows in the plasma sheet observed by Cluster, *Geophys. Res. Lett.*, *31*, L09894, doi:10.1029/2004GL019558.

Nakamura, R., A. Retin'o, W. Baumjohann, M. Volwerk, N. Erkaev, B. Klecker, E. A. Lucek, I. Dandouras, M. Andr'e, and Y. Khotyaintsev (2009), Evolution of dipolarization in the near-Earth current sheet induced by earthward-moving rapid flux transport, *Ann. Geophys.*, *27*, 1743–1754.

Northrop, T. G. (1963), Adiabatic charged-particle motion, *Rev. Geophys. Space Phys.*, *1*, 283–304.
Panov, E., et al. (2010), Multiple overshoot and rebound of a bursty bulk flow, *Geophys. Res. Lett.*, *37*, L08103, doi:10.1029/2009GL041971.
Pritchett, P. L., and F. V. Coroniti (2011), Plasma sheet disruption by interchange generated flow intrusions, *Geophys. Res. Lett.*, *38*, L10102, doi:10.1029/2011GL047527.
Runov, A., V. Angelopoulos, M. I. Sitnov, V. A. Sergeev, J. Bonnell, J. P. McFadden, D. Larson, K.-H. Glassmeier, and U. Auster (2009), THEMIS observations of an earthward-propagating dipolarization front?, *Geophys. Res. Lett.*, *36*, L14106, doi:10.1029/2009GL038980.
Runov, A., V. Angelopoulos, X.-Z. Zhou, X.-J. Zhang, S. Li, F. Plaschke, and J. Bonnell (2011), A THEMIS multicase study of dipolarization fronts in the magnetotail plasma sheet, *J. Geophys. Res.*, *116*, A05216, doi:10.1029/2010JA016316.
Runov, A., V. Angelopoulos, C. Gabrielse, X.-Z. Zhou, D. Turner, and F. Plaschke (2013), Electron fluxes and pitch-angle distributions at dipolarization fronts: THEMIS multipoint observations, *J. Geophys. Res. Space Physics*, *118*, 744–755, doi:10.1002/jgra.50121.
Sitnov, M. I., M. Swisdak, and A. V. Divin (2009), Dipolarization fronts as a signature of transient reconnection in the magnetotail, *J. Geophys. Res.*, *114*, A04202, doi:10.1029/2008JA013980.
Tang, C. L., Z. Y. Li, V. Angelopoulos, S. B. Mende, K. H. Glassmeier, E. Donovan, C. T. Russell, and L. Lu (2009), THEMIS observations of the near-Earth plasma sheet during a substorm, *J. Geophys. Res.*, *114*, A09211, doi:10.1029/2008JA013729.
Tang, C. L., V. Angelopoulos, A. Runov, C. T. Russell, H. Frey, K. H. Glassmeier, K. H. Fornacon, and Z. Y. Li (2010), Precursor activation and substorm expansion associated with observations of a dipolarization front by THEMIS, *J. Geophys. Res.*, *115*, A07215, doi:10.1029/2009JA014879.
Tang, C. L., L. Lu, M. Zhou, and Z. H. Yao (2013), THEMIS observations of electron acceleration associated with the evolution of substorm dipolarization in the near-Earth tail, *J. Geophys. Res. Space Physics*, *118*, 4237–4247, doi:10.1002/jgra.50418.
Tsyganenko, N. A. (1995), Modeling the Earth's magnetospheric magnetic field confined within a realistic magnetopause, *J. Geophys. Res.*, *100*, 5599–5612, doi:10.1029/94JA03193.
Wu, M. Y., Q. M. Lu, M. Volwerk, Z. Vörös, T. L. Zhang, L. C. Shan, and C. Huang (2013), A statistical study of electron acceleration behind the dipolarization fronts in the magnetotail, *J. Geophys. Res. Space Physics*, *118*, 4804–4810, doi:10.1002/jgra.50456.
Wu, P., T. A. Fritz, B. Larvaud, and E. Lucek (2006), Substorm associated magnetotail energetic electrons pitch-angle evolutions and flow reversals: Cluster observation, *Geophys. Res. Lett.*, *33*, L17101, doi:10.1029/2006GL026595.
Yang, J., F. R. Toffoletto, R. A. Wolf, and S. Sazykin (2011), RCM-E simulation of ion acceleration during an idealized plasma sheet bubble injection, *J. Geophys. Res.*, *116*, A05207, doi:10.1029/2010JA016346.
Yao, Z. H., et al. (2012), Mechanism of substorm current wedge formation: THEMIS observations, *Geophys. Res. Lett.*, *39*, L13102, doi:10.1029/2012GL052055.
Zhou, M., M. Ashour-Abdalla, X. Deng, D. Schriver, M. El-Alaoui, and Y. Pang (2009), THEMIS observation of multiple dipolarization fronts and associated wave characteristics in the near-Earth magnetotail, *Geophys. Res. Lett.*, *36*, L20107, doi:10.1029/2009GL040663.
Zhou, M., X. Deng, M. Ashour-Abdalla, R. Walker, Y. Pang, C. Tang, S. Huang, M. El-Alaoui, Z. Yuan, and H. Li (2013), Cluster observations of kinetic structures and electron acceleration within a dynamic plasma bubble, *J. Geophys. Res. Space Physics*, *118*, 674–684, doi:10.1029/2012JA018323.